Microporous and Mesoporous Materials 384 (2025) 113461

Contents lists available at ScienceDirect

Microporous and Mesoporous Materials

journal homepage: www.elsevier.com/locate/micromeso

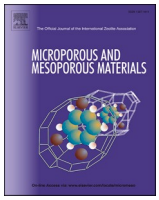

Intrusion-extrusion of water into-from hydrophobic nanopores at high temperature: Unexpected dependence of dewetting pressure above 200 °C

Cléophée Gourmand [a,*], Luis Bartolomé [a], Eder Amayuelas [a], Juan Miguel López del Amo [a], Elena Palomo del Barrio [a,b], Simone Meloni [c], Yaroslav Grosu [a,d,**]

[a] Centre for Cooperative Research on Alternative Energies (CIC energiGUNE), Basque Research and Technology Alliance (BRTA), Álava Technology Park, Albert Einstein 48, 01510, Vitoria-Gasteiz, Spain
[b] Ikerbasque - Basque Foundation for Science, María Díaz Haroko 3, 48013, Bilbao, Spain
[c] Department of Chemical, Pharmaceutical and Agricultural Sciences, University of Ferrara, Ferrara, 44121, Italy
[d] Institute of Chemistry, University of Silesia in Katowice, Szkolna 9 street, 40-006, Katowice, Poland

A B S T R A C T

Wetting of a porous solid by a fluid is of significant interest to many industrial processes. However, at the nanoscale, this process is complex, and little is known about its temperature dependance. In this work, we explored the intrusion-extrusion of water for a heterogeneous lyophobic system composed of a hydrophobic mesoporous silica gel and water over a wide 25–250 °C temperature range. The intrusion pressure was found to have a classical negative temperature dependance in the whole 25–250 °C temperature range. However, an unexpected non-monotonic temperature dependance was observed for the extrusion pressure. In particular, it became temperature independent above 200 °C. This observation suggests that dewetting of nanopores at high temperature is more complex than previously thought of and serves as experimental grounds for further theoretical exploration.

1. Introduction

When a system composed of a lyophobic porous material and a nonwetting liquid (heterogeneous lyophobic system) undergo sufficient compression/decompression, it exhibits intrusion-extrusion phenomena. This intrusion-extrusion of fluids into porous systems is of significant interest for many technological applications [1,2] such as chromatography and liquid separation [3–5], energetics [6–9] and porous material characterization [10,11]. Thus, the process has been studied on a wide range of hydrophobic materials such as aluminosilicates (zeolites) [8,12–15], silica gels [16–19] or metal-organic frameworks [6,20–24], mainly using liquid metals [10,18] aqueous solutions of salts [12,15,25,26] and water [6,14–24].

Although it is widely used, the intrusion-extrusion process is not fully understood. One of the points lacking understanding is the effect of temperature, particularly at high temperatures. Indeed, this process tends to be temperature dependent. Understanding and controlling this dependence could be of great interest for classical intrusion-extrusion applications such as shock-absorbers [17–19,27,28], as well as for emerging ones like thermal actuation [29] and thermal energy storage [8,30–32]. However, these effects tend to be overlooked, as most studies focus on a small temperature range, mostly until 80–90 °C and with few data points [12,13,17,18,21]. Most of the studies about intrusion-extrusion temperature dependance have highlighted a decrease of intrusion pressure with temperature, which fits the capillary theory [16,17,33]. The opposite case has hardly been observed and exclusively for microporous materials such as MOFs or zeolite Y [6,12,33]. For extrusion, the temperature dependance was more complex and other theories such as nucleation theory, line tension and critical bubble nucleation are needed to understand the extrusion process [16,17,28].

Very few studies have been done on a wider temperature range. Grosu et al. studied a {C8 hydrophobic silica gel + water} system until 150 °C [16] and Merchiori et al. have worked on water confinement in a Cu_2tebpz (tebpz = 3,3′,5,5′-tetraethyl-4,4′-bipyrazolate) hydrophobic MOF until 170 °C [6,33]. Both works highlighted a change in the temperature dependance of the intrusion or extrusion pressure. In the former, the extrusion pressure was found to switch its temperature dependance from positive to negative around 100 °C. This was explained

* Corresponding author.
** Corresponding author. Centre for Cooperative Research on Alternative Energies (CIC energiGUNE), Basque Research and Technology Alliance (BRTA), Álava Technology Park, Albert Einstein 48, 01510, Vitoria-Gasteiz, Spain.
E-mail addresses: cgourmand@cicenergigune.com (C. Gourmand), ygrosu@cicenergigune.com (Y. Grosu).

https://doi.org/10.1016/j.micromeso.2024.113461
Received 8 November 2024; Received in revised form 12 December 2024; Accepted 14 December 2024
Available online 15 December 2024
1387-1811/© 2025 The Authors. Published by Elsevier Inc. This is an open access article under the CC BY license (http://creativecommons.org/licenses/by/4.0/).

by a change in the dominant phenomena driving the extrusion from critical bubble nucleation to capillary forces [16]. In the second work, the intrusion pressure was found to change its temperature dependance from positive to negative around 107°C. This change was explained by two phenomena involving the water vapor pressure inside the MOF pores and the water surface tension [6,33]. For this material, the authors have also highlighted a phase transition to confined supercritical water at temperatures ≈250 °C below bulk critical temperature. Overall, studies at temperatures higher than 100 °C have shown a non-monotonic trend of intrusion-extrusion pressures. Thus, intrusion-extrusion studies at high temperatures may reveal non-monotonic behaviors crucial for application and fundamental understanding of lyophobic nanoporous materials wetting-dewetting process [16].

In this work, we studied the water intrusion-extrusion phenomenon for a {C8 hydrophobic silica gel + water} system. This system was based on a silica gel of average pore size of 60Å, functionalized with octyl groups. Water intrusion-extrusion was performed on a 25–250 °C temperature range. To our knowledge, it is the first time water intrusion-extrusion is performed on such temperature range and paves the way for further applications of {hydrophobic silica + water} systems. This paper describes the behaviour of the {C8 hydrophobic silica gel + water} system and its stability at high temperature and high pressure. Experimental data highlighted an unexpected and complex temperature dependance for extrusion in the previously unexplored temperature range.

2. Experimental section

2.1. Reagents

All reagents were obtained from commercial sources and were used without further purification. These reagents were silica gel 60 Å (W. R. Grace – Davisil), octyltrichlorosilane (OTCS, Thermoscientific, 97 %) and toluene (Sigma-Aldrich, ≥99.5 %).

2.2. Functionalization of silica gel by octyl groups

For the hydrophobization of silica, octyl (C8) groups were covalently grafted on silica gel with 60 Å pore size. The grafting protocol was inspired from Martin et al. [34] 1 g of silica gel were suspended in 30 mL toluene at room temperature. Octyltrichlorosilane (4 mol OTCS/nm^2) were added and after 1 h of stirring, H_2O (3 mol H_2O/mol octyltrichlorosilane) was added. Then the reaction was let to stir 1 h at room temperature, 21 h at 60 °C and 4 h at 100 °C. The solid was recovered by filtration and dried. Finally, the sample was activated overnight at 140 °C, 20 mbar to remove ungrafted groups. The materials will be thereafter referred to as *SiO_2* and *SiO_2-C8*.

2.3. Characterization techniques

Specific surface area, pore size and volume have been determined by N_2 physisorption at 77 K. Prior to the measurement, the mesoporous silica samples were outgassed under vacuum at 130 °C for 20 h. Measurements were performed with a Micromeritics ASAP 2460 surface analyzer. Specific surface area was calculated from the BET equation, in the P/P_0 = 0.05–0.25 pressure range. Pore size distributions were obtained from the Broekhoff and de Boer (BdB) model on the desorption branch. Pore volume was determined at P/P_0 = 0.99. To qualitatively assess the hydrophobicity of the material, BET constant C_{BET}, related to the heat of adsorption, was calculated from the BET equation in its linear range (P/P_0 = 0.05–0.25):

$$\frac{P/P_0}{n\left(1-P/P_0\right)} = \frac{1}{n_m C_{BET}} + \frac{(C_{BET}-1)}{n_m C_{BET}} \times \frac{P}{P_0} \quad \text{(Eq.1)}$$

in which P/P_0 is the relative equilibrium pressure, n is the amount adsorbed, n_m the monolayer capacity.

Thermogravimetric analysis (TGA) was performed to estimate easily the grafting density. TGA was carried out using Netzsch TG 209 F1 Libra under N_2 flow or air flow from room temperature to 1000 °C with a heating rate of 10 °C/min. Grafting density was estimated from the total mass loss obtained.

Solid-state NMR was used to study the material before and after water intrusion-extrusion. All experiments were recorded using a Brucker Avance III 500 MHz spectrometer. Samples were packed inside 2.5 mm rotors and magic angle spinning (MAS) speed was fixed at 20 kHz in all experiments. The rotors were spun in a nitrogen atmosphere, to avoid possible reactions with moisture during the experiment. The ^{13}C spectra were recorded using one pulse excitation with a pulse length of 2.9 μs and 784 scans were accumulated with a recycle delay of 10s. The ^{1}H-^{29}Si spectra were obtained using a standard 1D cross-polarization (CP) experiment with a 75–100 ramped contact time of 1 ms, a recycle delay of 3s and 80k scans.

2.4. Water intrusion-extrusion experiments at room temperature

The functionalized silica was mixed with pure water and encapsulated in flexible hermetic capsules. Water intrusion-extrusion tests at room temperature were performed by means of water porosimetry using an Autopore IV 9500 porosimeter (Micromeritics). In each experiment, the penetrometer was evacuated to a pressure less than 5 Pa and filled with mercury. The system was compressed to 150 MPa and decompressed to observe the intrusion-extrusion phenomenon. The material was evaluated over 4 intrusion-extrusion cycles.

2.5. PVT setup

The PV isotherms at different temperatures were measured using CICenergiGUNE's PVT setup [20]. Briefly, this setup consists of piston drive module and a high-pressure syringe connected (high-pressure variable volume unit) to a cylindric metallic vessel which the encapsulated samples are tested. For these experiments, SiO_2-C8 was encapsulated and placed in the PVT reactor. Two types of capsules were used: one made with Teflon and a metallic one. In the pressurization cycles, pressure was varying from 1 to 600 bar. To ensure not having boiling water inside the vessel, the minimal pressure for each experiment was fixed above the vapor pressure of water at the said temperature. Tests were conducted at temperatures varying from 25 to 250 °C, every 25 °C. To allow reaching temperatures as high as 250 °C, a heating jacket (Eurotechnica), increasing the temperature electrically, was used. The temperature was controlled by a heating control and a thermocouple placed in the vessel. To ensure SiO_2-C8 does not degrade with temperature and pressure, three cycles were performed for some of the highest temperatures.

3. Results and discussion

3.1. SiO_2 functionalization

Before functionalization, Davisil 60 Å (6 nm diameter pores) is a mesoporous silica featuring disordered pores of average diameter 6 nm, large enough to accommodate octyl groups. N_2 adsorption isotherms are presented on Fig. 1 (A). For both the grafted and pristine silica, N_2 physisorption on this material led to a type IV isotherm with a type 2 hysteresis, typical of solid with complex pore structure and important network effects.

After grafting, the specific surface area decreased from 566 to 246 m^2 g^{-1} and the pore volume decreased from 0.834 to 0.279 cm^3. g^{-1}. One specific feature of Davisil 60 Å is its wide pore size distribution, centered on 6 nm. After grafting, this pore size distribution (Fig. 1 (B)) is

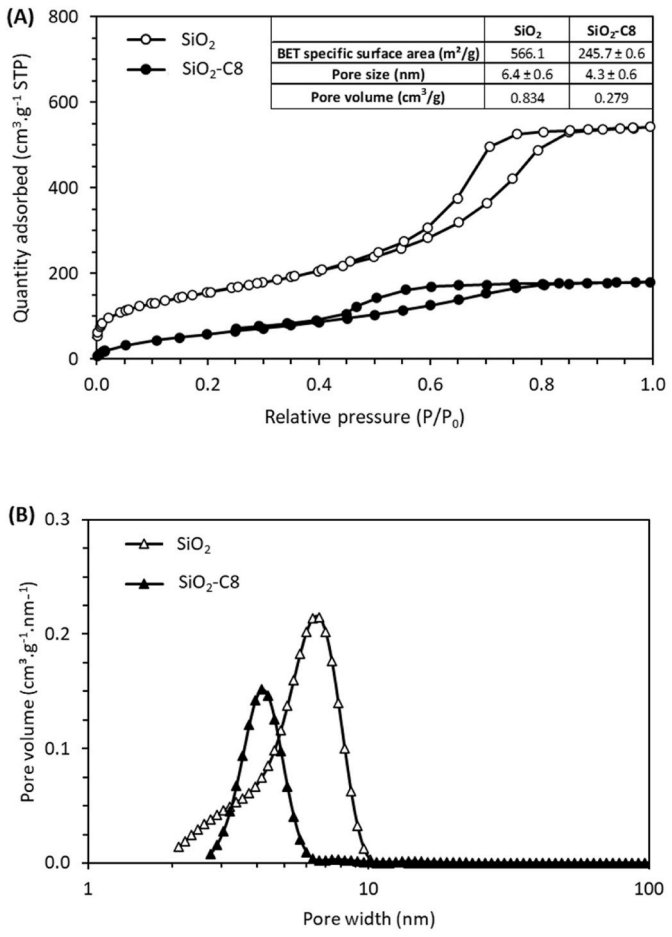

Fig. 1. (A) N_2 adsorption isotherms of SiO_2 (empty circles) and SiO_2-C8 (plain circles) and (B) BdB pore size distribution for SiO_2 (empty triangles) and SiO_2-C8 (plain triangles).

shifted towards smaller pore sizes and gets narrower, highlighting a potential influence of pore size distribution in the grafting. In some studies, the BET constant C_{BET} has been used as an indicator to assess qualitatively the surface energies [34–36]. For the pristine SiO_2, C_{BET} was around 85, which highlights the presence of polar groups, in this case silanol. After functionalization, C_{BET} decreases to 56. Typically, silica grafted with alkyl chains show C_{BET} constants between 15 and 25 [35]. This intermediate value thus highlights an incomplete surface coverage, most likely due to the presence of accessible silanol groups. These silanols can be either residual surface silanols from the silica or formed from the incomplete condensation of OTCS.

Grafting densities were estimated from thermogravimetric analysis (Fig. 2). As mentioned above, SiO_2-C8 contains polar Si-OH groups, which can condensate above 200 °C, generating a mass loss, which could slightly influence the estimation of the grafting density [37]. For our silica gel, Si-OH condensation led to mass loss of 2.6 % under N_2 and 2.4 % under air, which happened between 200 and 600 °C. SiO_2-C8 showed a unique decomposition step with a mass loss of 19 % starting around 420 °C in N_2 and around 250 °C in air. This corresponds to a grafting quantity of 0.24 g_{octyl}/g_{SiO2} or a grafting density of 1.8 octyl groups/nm^2. Considering the possible influence of polar Si-OH groups in the mass loss, it is possible to affirm that the real grafting density is in the 1.7–1.8 octyl groups/nm^2 range.

3.2. Water intrusion-extrusion at room temperature

The H_2O intrusion-extrusion performance of SiO_2-C8 was evaluated over 4 intrusion-extrusion cycles.

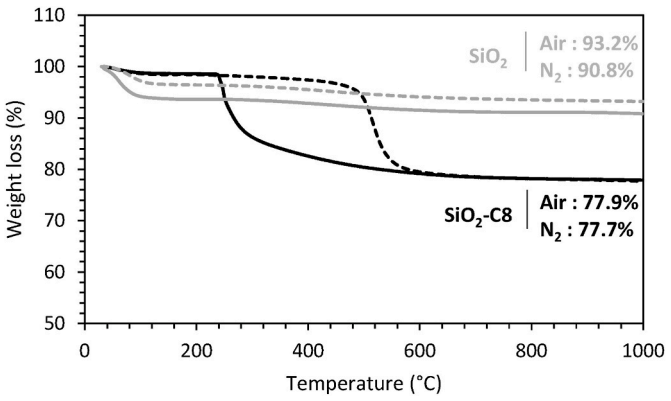

Fig. 2. Thermogravimetric analysis of SiO_2 (grey line) and SiO_2-C8 (black line) in N_2 (dashed line) and air (solid line).

Pressure-volume (PV) isotherms are presented on Fig. S1 (A). A great reproducibility is observed between the cycles. These results show a high stability of SiO_2-C8 material over the cycles. This is highlighted in Fig. S1 (B) in which it can be seen that, for all four cycles, intrusion started at P = 30.0 MPa and reached its maximum at P = 38.5 MPa. Extrusion started around 25 MPa. The peak of extrusion was reached at 5 MPa. 0.14 ± 0.01 mL of water per gram of material were intruded and extruded in each cycle, highlighting the stability of SiO_2-C8. This value corresponds to half of the pore volume measured by N_2 adsorption. This difference could be explained by the presence of accessible hydrophilic groups (Si-OH) mentioned before and to the lower water density under hydrophobic nanoconfinement.

3.3. Water intrusion-extrusion at different temperatures

With this data in hand, water intrusion-extrusion experiments inside the pores of SiO_2-C8 were performed between 25 °C and 250 °C. To our knowledge, it is the first time that water intrusion-extrusion experiments have been done on such a temperature range.

PV-isotherms are presented on Fig. 3 (A). For a better visibility, isotherms are shifted on the X-axis. On Fig. S2, the hysteresis are superposed to allow a better comparison.

The derivative dP/dV (Fig. 3 (B) and 3 (C)) highlights variations in the intrusion and extrusion pressure as a function of temperature. This variation is represented in Fig. 4(A and B). The derivative also highlights variations in the intrusion and extrusion volume, obtained by integration of the intrusion and extrusion peaks, respectively. It can be observed that the intrusion volume is stable until 200 °C and then subsequently decreases by 20 % at temperatures higher than 200 °C (Fig. 4 (C)).

The hysteresis area overall decreases with increasing temperature from ≈6 J g^{-1} at 25 °C to ≈2 J g^{-1} at 250 °C (Fig. 4 (D)).

It can be observed that the intrusion pressure decreases with increasing temperature. This behaviour is the most common one and has been observed for {hydrophobic silica + water} systems [16].

This shows that the intrusion pressure follows the Laplace-Washburn equation (Eq. (2)), as for most liquids, the temperature derivatives of the surface tension dγ/dT and contact angle dθ/dT are negative.

$$P_{int,ext} = -\frac{2\gamma \cos\theta}{r} \quad \text{(Eq. 2)}$$

in which P_{int} is the (intrusion or extrusion) pressure, γ is the surface tension, θ is the contact angle and r the pore radius.

In contrast to the intrusion process, the evolution of extrusion pressure with the temperature is very different. Until 100 °C, the extrusion pressure increases with temperature. Then, it decreases until 200 °C. Such behaviour is consistent with previously reported {SiO_2-C8 +

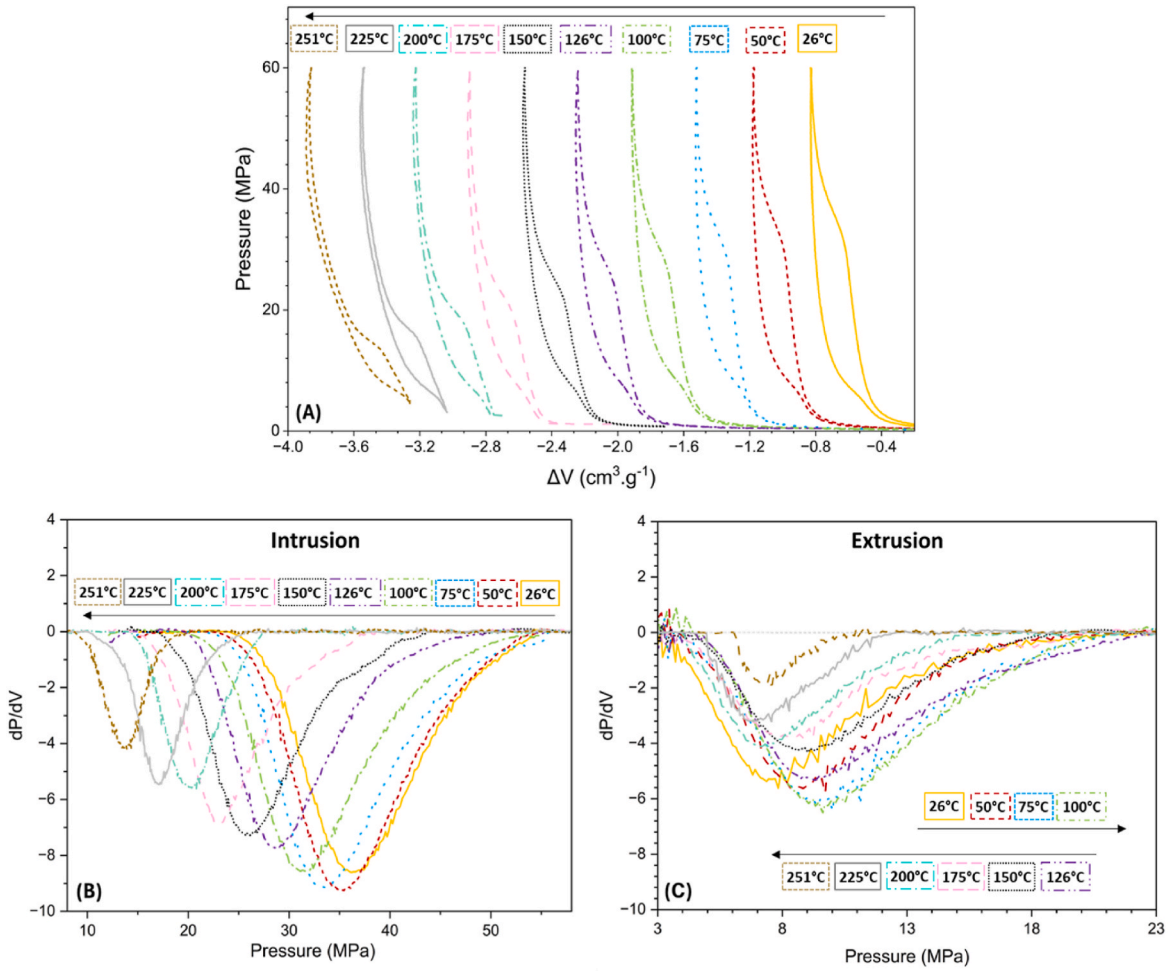

Fig. 3. H_2O intrusion-extrusion for SiO_2-C8 for different temperatures (A) PV isotherms (shifted on the X-axis), (B) dP/dV derivative for intrusion, (C) dP/dV derivative for extrusion.

water} system recorder up to 150 °C using silica of larger pore size [16]. Unexpectedly, further temperature increase does not lead to reduction of the extrusion pressure, that instead stabilizes and remains constant within the error of the experiment until 250 °C.

A test of cyclability has been done at 250 °C. 3 successive intrusion and extrusion cycles from 2 to 60 MPa have been performed. Very few variations were observed between the cycles as it can be seen on Fig. S4, highlighting a certain stability of the material in these conditions. Indeed, the intrusion and extrusion pressures varied of ±0.4 MPa and the intruded and extruded volume of ±0.01 mL g^{-1}. This suggest that the observed non-monotonic trend cannot be explained by the material degradation. To ensure no degradation of the grafting happened, TGA analysis was performed on the material after high-temperature intrusion-extrusion cycling in the 25–250 °C range (Fig. S3). No apparent degradation of the organic grafting was observed, and the grafting density stays in the 1.7–1.8 groups/nm^2 range.

After cycling, water intrusion-extrusion at room temperature was performed to see the influence of cycling at high temperatures on the material (Fig. S5). A reduction in intrusion pressure has been observed but the intrusion volume remains unchanged, 0.14 ± 0.01 $mL_{H2O}.g^{-1}$.

No extrusion is clearly visible on the isotherm (most likely because $P_{ext} < P_{atm}$) which, according to TGA data, cannot be attributed to grafting degradation. A control experiment was also performed by ^{13}C solid state NMR to check the integrity of the octyl chains (Fig. S6). No apparent change has been observed before and after the test, confirming the results obtained with TGA. However, there are different possible hypothesis. Indeed, the intrusion barrier is the pore mouth and the extrusion depends on the interior of the pore. Thus, it is highly possible that interior of the pores was affected. One possible factor would be the silanol content/defects of the material. Indeed, after having spent some time in water at high pressure and high temperature, some siloxane bridges could have broken, thus creating defects. This has been investigated using ^{1}H- ^{29}Si CP MAS NMR (Fig. S7). In this experiment, magnetization is transferred from ^{1}H to nearby ^{29}Si isotopes, in order to enhance the signal from possible SiOH functional groups at the surface. Results have shown that after the test at 250 °C, a Q^3 peak, typical of free and vicinal silanols appears, showing that some of the siloxane bridges have been hydrolyzed.

Water intrusion-extrusion at room temperature was performed again after a regeneration step (15 h at 200 °C under vacuum). This time, intrusion pressure was still lower compared to non-cycled silica, however, increased slightly compared to non-regenerated cycled silica. The intrusion volume remained unchanged (i.e. within the standard deviation) but a slight extrusion, corresponding to 7 % of the intruded volume was observed at ≈ 6 MPa. Such effect of regenerative step may suggest that silanol formation may be behind the reduced hydrophobicity of the silica after the cycling. This hypothesis would of course be relevant only in the case when intruded water touches silica despite hydrophobic grafting. Due to high inhomogeneity of water in such grafted silica systems this scenario is possible [38]. Such possible silanol formation cannot explain the non-monotonic trend of extrusion pressure at temperatures above 200 °C, as increase in hydrophilicity of silica should have resulted in further lowering of the extrusion pressure, not its stabilization with temperature.

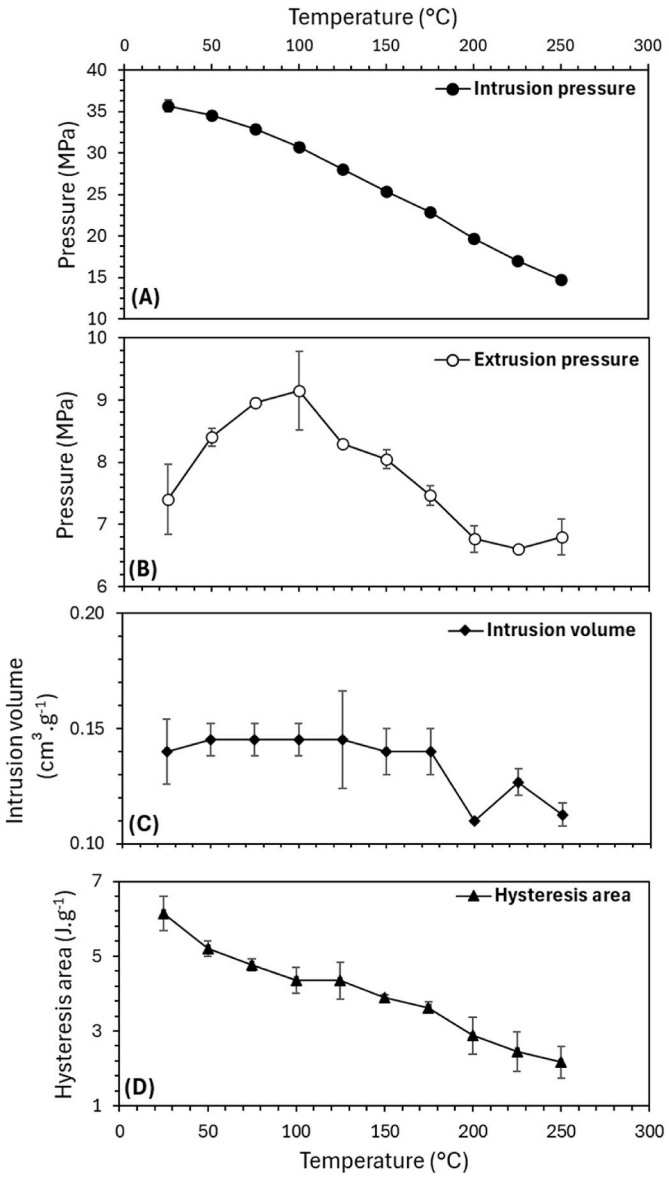

Fig. 4. Temperature dependance of some key parameters (A) intrusion pressure, (B) extrusion pressure, (C) intrusion volume and (D) hysteresis area.

It is of interest to mention that this lack of thermal stability in water has also been observed for many silica-based hydrophobic materials used in chromatography [39]. There are indeed other more stable candidates, containing for instance bridged organic groups [40], polymer coatings [41,42] or other inorganic materials such as graphitized carbon or metal oxides such as ZrO_2, TiO_2 and Al_2O_3 [42,43]. However, achieving intrusion-extrusion is very challenging and deserves a separate study.

In this final part of the manuscript, we discuss some hypotheses that may explain why extrusion pressure presents three regimes with temperature: ascending, descending and stationary. The objective is to promote discussion within the community about the dependence of extrusion (and intrusion) pressure with temperature, considering that the phenomenology might depend – qualitatively and quantitatively – on the chemical, morphological and geometrical characteristics of the porous material. The first point to remark on is that for the extrusion pressure no equation exists that can predict its value, neither for macroscopic nor for microscopic system. Nevertheless, at a qualitative level one can formulate extrusion as a confined nucleation process, where a vapor or gas bubble forms and/or expands, pushing out the liquid filling the cavities of the porous material [44,45]. Before proceeding to discuss any hypothesis on the peculiar trend of P_{ext} it is necessary to recall another observation, that in heterogeneous hydrophobic systems, hydrophobic gasses dissolved in the liquid, e.g., N_2, O_2, etc, are attracted to the solids' pores [46] to minimize the disruption of the hydrogen bond network of the liquid [47]. Thus, one expects that upon intrusion, these gases are trapped in the cavities and a temperature increase results in a corresponding increase of the gas pressure. A higher pressure of gasses trapped in the cavities make it easier for liquid extrusion, hence increases P_{ext}. Remarkably, a similar process has been observed associated to only water vapor in the cavities: the confined vapor pressure is much larger than the bulk counterpart at the same temperature, reaching up to several MPa at relatively low temperatures in hydrophobic MOFs [33]. Temperature also has an effect on other characteristics of the confined system, which affect P_{ext} in non-trivial ways. At higher temperatures the surface tension of water decreases, making confined nucleation easier. This contributes to increase P_{ext}. However, temperature increases also reduce the hydrophobicity of the material (contact angle and surface tension of water reduction), which amounts to an additional force to be overcome to extrude the liquid. We believe that the non-monotonic trend of the extrusion pressure is because of the temperature favoring formation and or/growth of vapor and/or gas bubbles at low temperature, and the competing mechanism of liquid retention due to reduction of hydrophobicity overcoming the other at higher temperatures [16]. Concerning the stationary region of the extrusion pressure at temperatures above 200 °C, we have no intuitive argument to propose to explain this observation. Here, we just recall that recent calculations on the *internal* contact angle (θ_{int}) of a hydrophobic MOF revealed that beyond some threshold temperature, θ_{int} is almost constant (see Fig. 2a of Ref. [33]).

To the best of our knowledge a novel phenomenology reported for the first time in this manuscript is the different qualitative dependence of the intrusion and extrusion pressure with temperature: the former decreases monotonically, the second has the non-monotonic trend extensively discussed in the previous paragraph. The widely accepted idea that the two processes, intrusion and extrusion, should be qualitatively affected in the same way by any effect biasing the system, here the temperature, is rooted on a quasi-static picture of the intrusion/extrusion process: one just follows the same path as the other in the opposite direction. Indeed, early works investigating intrusion/extrusion within the rigorous framework of the atomistic and continuum statistical mechanics of rare events are based on this quasi-static picture [44,48,49]. However, it has been shown that for porous systems of suitable size (not too small) the dynamics is dominated by viscous processes, and for porous systems that are not too big, the effect of confinement is negligible. A dynamic picture beyond the classical quasi-static framework is needed to describe intrusion/extrusion [50]. Within this dynamical picture, the intrusion and extrusion path are different, for example intrusion is controlled by the external hydrophobicity, and extrusion from the internal one, and under conditions of high confinement might be significantly different.

4. Conclusions

In this work, the temperature dependance of a heterogeneous lyophobic system {C8 hydrophobic silica gel + water} has been studied. Octyl (C8) groups have successfully been grafted on a commercial silica gel with 6 nm pores, reducing pore size from 6 to 4 nm. Water intrusion-extrusion experiments have been performed successfully until 250 °C. At this temperature, the material showed reproducible PV isotherms over 3 intrusion-extrusion cycles, although PV isotherms at room temperature showed significant changes after exposure to water at 250 °C, due to changes in the surface of the material (hydrolysis of siloxanes). The temperature dependance of the extrusion pressure was found to be non-monotonic and unexpected in the previously unexplored temperature range. In particular, at temperatures higher than 200 °C, it was

demonstrated to be temperature independent. This observation reveals a more complex mechanism of dewetting of hydrophobic nanopores at high temperature and requires additional theoretical considerations to be explained. Hypotheses to explain the complex trend of the extrusion pressure on the temperature, and the difference in the effect of this external parameter on intrusion and extrusion, are discussed. These hypotheses must be understood as a possible starting point to promote the discussion within the community, rather than as the best explanation to the experimental evidence presented in the manuscript.

CRediT authorship contribution statement

Cléophée Gourmand: Writing – original draft, Visualization, Investigation, Formal analysis. **Luis Bartolomé:** Investigation. **Eder Amayuelas:** Investigation. **Juan Miguel López del Amo:** Investigation, Validation, Writing – review & editing. **Elena Palomo del Barrio:** Supervision. **Simone Meloni:** Writing – review & editing, Writing – original draft, Investigation. **Yaroslav Grosu:** Writing – review & editing, Supervision, Methodology, Conceptualization.

Declaration of competing interest

The authors declare that they have no known competing financial interests or personal relationships that could have appeared to influence the work reported in this paper.

Acknowledgments

This publication is part of the R&D project PID2023-148734OA-I00 funded by MCIU/AEI/10.13039/501100011033 and by EDRF, EU. This article is part of the grant RYC2021- 032445-I funded by MICIN/AEI/10.13039/501100011033 and by the European Union NextGenerationEU/PRTR.

Appendix A. Supplementary data

Supplementary data to this article can be found online at https://doi.org/10.1016/j.micromeso.2024.113461.

Data availability

Data will be made available on request.

References

[1] A. Giacomello, C.M. Casciola, Y. Grosu, S. Meloni, Liquid intrusion in and extrusion from non-wettable nanopores for technological applications, Eur. Phys. J. B 94 (8) (2021) 1–24, https://doi.org/10.1140/EPJB/S10051-021-00170-3, 2021 94.

[2] A. Le Donne, A. Tinti, E. Amayuelas, H.K. Kashyap, G. Camisasca, R.C. Remsing, R. Roth, Y. Grosu, S. Meloni, Intrusion and extrusion of liquids in highly confining media: bridging fundamental research to applications, Adv. Phys. X 7 (2022) 2052353, https://doi.org/10.1080/23746149.2022.2052353.

[3] F. Gritti, D. Brousmiche, M. Gilar, T.H. Walter, K. Wyndham, Kinetic mechanism of water dewetting from hydrophobic stationary phases utilized in liquid chromatography, J. Chromatogr. A 1596 (2019) 41–53, https://doi.org/10.1016/j.chroma.2019.02.051.

[4] S.R. Bakalyar, M.P.T. Bradley, R. Honganen, The role of dissolved gases in high -performance liquid chromatography, J. Chromatogr. A 158 (1978) 277–293, https://doi.org/10.1016/S0021-9673(00)89973-2.

[5] A.K. Kota, G. Kwon, W. Choi, J.M. Mabry, A. Tuteja, Hygro-responsive membranes for effective oil–water separation, Nat. Commun. 3 (1) (2012) 1–8, https://doi.org/10.1038/ncomms2027, 2012 3.

[6] S. Merchiori, A. Le Donne, J.D. Littlefair, A.R. Lowe, J.J. Yu, X.D. Wu, M. Li, D. Li, M. Geppert-Rybczyńska, L. Scheller, B.A. Trump, A.A. Yakovenko, P. Zajdel, M. Chorążewski, Y. Grosu, S. Meloni, Mild-temperature supercritical water confined in hydrophobic metal-organic frameworks, J. Am. Chem. Soc. 146 (2024) 13236–13246, https://doi.org/10.1021/jacs.4c01226.

[7] Y. Grosu, M. Mierzwa, V.A. Eroshenko, S. Pawlus, M. Chorazewski, J.M. Nedelec, J. P.E. Grolier, Mechanical, thermal, and electrical energy storage in a single working body: electrification and thermal effects upon pressure-induced water intrusion-extrusion in nanoporous solids, ACS Appl. Mater. Interfaces 9 (2017) 7044–7049, https://doi.org/10.1021/acsami.6b14422.

[8] V. Eroshenko, R.C. Regis, M. Soulard, J. Patarin, Energetics: a new field of applications for hydrophobic zeolites, J. Am. Chem. Soc. 123 (2001) 8129–8130, https://doi.org/10.1021/ja011011a.

[9] C.V. Suciu, K. Yaguchi, Endurance tests on a colloidal damper destined to vehicle suspension, Exp. Mech. 49 (2009) 383–393, https://doi.org/10.1007/s11340-008-9163-z.

[10] J. Rouquerol, G. Baron, R. Denoyel, H. Giesche, J. Groen, P. Klobes, P. Levitz, A. V. Neimark, S. Rigby, R. Skudas, K. Sing, M. Thommes, K. Unger, Liquid intrusion and alternative methods for the characterization of macroporous materials (IUPAC technical report), Pure Appl. Chem. 84 (2012) 107–136, https://doi.org/10.1351/PAC-REP-10-11-19.

[11] B. Coasne, A. Galarneau, F. Di Renzo, R.J.M. Pellenq, Intrusion and retraction of fluids in nanopores: effect of morphological heterogeneity, J. Phys. Chem. C 113 (2009) 1953–1962, https://doi.org/10.1021/jp807828a.

[12] A. Han, W. Lu, T. Kim, V.K. Punyamurtula, Y. Qiao, The dependence of infiltration pressure and volume in zeolite Y on potassium chloride concentration, Smart Mater. Struct. 18 (2009) 024005, https://doi.org/10.1088/0964-1726/18/2/024005.

[13] Y. Qiao, V.K. Punyamurtula, A. Han, X. Kong, F.B. Surani, Temperature dependence of working pressure of a nanoporous liquid spring, Appl. Phys. Lett. 89 (2006), https://doi.org/10.1063/1.2408664.

[14] O.V. Ievtushenko, V.A. Eroshenko, Y.G. Grosu, J.M. Nedelec, J.P.E. Grolier, Evolution of the energetic characteristics of {silicalite-1 + water} repulsive clathrates in a wide temperature range, Phys. Chem. Chem. Phys. 15 (2013) 4451–4457, https://doi.org/10.1039/C3CP44587A.

[15] L. Ronchi, H. Nouali, T.J. Daou, J. Patarin, A. Ryzhikov, Heterogeneous lyophobic systems based on pure silica ITH-type zeolites: high pressure intrusion of water and electrolyte solutions, New J. Chem. 41 (2017) 15087–15093, https://doi.org/10.1039/C7NJ03470A.

[16] Y. Grosu, O. Ievtushenko, V. Eroshenko, J.M. Nedelec, J.P.E. Grolier, Water intrusion/extrusion in hydrophobized mesoporous silica gel in a wide temperature range: capillarity, bubble nucleation and line tension effects, Colloids Surf. A Physicochem. Eng. Asp. 441 (2014) 549–555, https://doi.org/10.1016/j.colsurfa.2013.10.022.

[17] L. Guillemot, T. Biben, A. Galarneau, G. Vigier, É. Charlaix, Activated drying in hydrophobic nanopores and the line tension of water, Proc. Natl. Acad. Sci. U.S.A. 109 (2012) 19557–19562, https://doi.org/10.1073/pnas.1207658109.

[18] L. Guillemot, A. Galarneau, G. Vigier, T. Abensur, É. Charlaix, New device to measure dynamic intrusion/extrusion cycles of lyophobic heterogeneous systems, Rev. Sci. Instrum. (2012), https://doi.org/10.1063/1.4754631.

[19] A.Y. Fadeev, V.A. Eroshenko, Study of penetration of water into hydrophobized porous silicas, J. Colloid Interface Sci. 187 (1997) 275–282, https://doi.org/10.1006/jcis.1996.4495.

[20] E. Amayuelas, L. Bartolomé, Y. Zhang, J.M. López del Amo, O. Bondarchuk, A. Nikulin, F. Bonilla, E.P. del Barrio, P. Zajdel, Y. Grosu, Quality-dependent performance of hydrophobic ZIF-67 upon high-pressure water intrusion–extrusion process, Phys. Chem. Chem. Phys. 26 (2024) 2440–2448, https://doi.org/10.1039/D3CP03519K.

[21] Y. Grosu, G. Renaudin, V. Eroshenko, J.M. Nedelec, J.P.E. Grolier, Synergetic effect of temperature and pressure on energetic and structural characteristics of {ZIF-8 + water} molecular spring, Nanoscale 7 (2015) 8803–8810, https://doi.org/10.1039/C5NR01340B.

[22] L.J.W. Johnson, D. Mirani, A. Le Donne, L. Bartolomé, E. Amayuelas, G.A. López, G. Grancini, M. Carter, A.A. Yakovenko, B.A. Trump, S. Meloni, P. Zajdel, Y. Grosu, Effect of crystallite size on the flexibility and negative compressibility of hydrophobic metal-organic frameworks, Nano Lett. 23 (2023) 10682–10686, https://doi.org/10.1021/acs.nanolett.3c02431.

[23] E. Amayuelas, J. Farrando-Perez, A. Missyul, Y. Grosu, J. Silvestre-Albero, C. Carrillo-Carrión, Fluorinated nanosized zeolitic-imidazolate frameworks as potential devices for mechanical energy storage, ACS Appl. Mater. Interfaces 16 (2024) 46374–46383, https://doi.org/10.1021/acsami.4c09969.

[24] I. Khay, G. Chaplais, H. Nouali, G. Ortiz, C. Marichal, J. Patarin, Assessment of the energetic performances of various ZIFs with SOD or RHO topology using high pressure water intrusion–extrusion experiments, Dalton Trans. 45 (2016) 4392–4400, https://doi.org/10.1039/C5DT03486H.

[25] A. Han, W. Lu, T. Kim, X. Chen, Y. Qiao, Influence of anions on liquid infiltration and defiltration in a zeolite Y, Phys. Rev. 78 (2008) 031408, https://doi.org/10.1103/PhysRevE.78.031408.

[26] M. Pillot, B. Lebeau, H. Nouali, T.J. Daou, J. Patarin, A. Ryzhikov, High pressure intrusion of water and LiCl aqueous solutions in hydrophobic KIT-6 mesoporous silica: influence of the grafted group nature, Microporous Mesoporous Mater. 280 (2019) 248–255, https://doi.org/10.1016/j.micromeso.2019.02.006.

[27] N. Gokulakrishnan, J. Parmentier, M. Trzpit, L. Vonna, J.L. Paillaud, M. Soulard, Intrusion/extrusion of water into organic grafted SBA-15 silica materials for energy storage, J. Nanosci. Nanotechnol. 13 (2013) 2847–2852, https://doi.org/10.1166/jnn.2013.7405.

[28] B. Lefevre, A. Saugey, J.L. Barrat, L. Bocquet, E. Charlaix, P.F. Gobin, G. Vigier, Intrusion and extrusion of water in hydrophobic mesopores, J. Chem. Phys. 120 (2004) 4927–4938, https://doi.org/10.1063/1.1643728.

[29] M. Chorążewski, P. Zajdel, T. Feng, D. Luo, A.R. Lowe, C.M. Brown, J.B. Leão, M. Li, M. Bleuel, G. Jensen, D. Li, A. Faik, Y. Grosu, Compact thermal actuation by water and flexible hydrophobic nanopore, ACS Nano 15 (2021) 9048–9056, https://doi.org/10.1021/acsnano.1c02175.

[30] A.R. Lowe, P. Ślęczkowski, E. Arkan, A. Le Donne, L. Bartolomé, E. Amayuelas, P. Zajdel, M. Chorążewski, S. Meloni, Y. Grosu, Exploring the heat of water intrusion into a metal-organic framework by experiment and simulation, ACS Appl.

Mater. Interfaces 16 (2024) 5286–5293, https://doi.org/10.1021/acsami.3c15447.
[31] L. Bartolomé, A. Anagnostopoulos, A.R. Lowe, P. Ślęczkowski, E. Amayuelas, A. Le Donne, M. Wasiak, M. Chorążewski, S. Meloni, Y. Grosu, Tuning wetting-dewetting thermomechanical energy for hydrophobic nanopores via preferential intrusion, J. Phys. Chem. Lett. 15 (2024) 880–887, https://doi.org/10.1021/acs.jpclett.3c03330.
[32] G. Fraux, F.X. Coudert, A. Boutin, A.H. Fuchs, Forced intrusion of water and aqueous solutions in microporous materials: from fundamental thermodynamics to energy storage devices, Chem. Soc. Rev. 46 (2017) 7421–7437, https://doi.org/10.1039/C7CS00478H.
[33] S. Merchiori, A. Le Donne, R. Bhatia, M. Alvelli, J.J. Yu, X.D. Wu, M. Li, D. Li, L. Scheller, A.R. Lowe, M. Geppert-Rybczynska, B.A. Trump, A.A. Yakovenko, M. Chorążewski, P. Zajdel, Y. Grosu, S. Meloni, Counterintuitive trend of intrusion pressure with temperature in the hydrophobic Cu2(tebpz) MOF, Small (2024) 2402173, https://doi.org/10.1002/smll.202402173.
[34] T. Martin, A. Galarneau, D. Brunel, V. Izard, V. Hulea, A.C. Blanc, S. Abramson, F. Di Renzo, F. Fajula, Towards total hydrophobisation of MCM-41 type silica surface, Stud. Surf. Sci. Catal. 135 (2001) 178–185, https://doi.org/10.1016/S0167-2991(01)81330-6.
[35] F. Bernardoni, A.Y. Fadeev, Adsorption and wetting characterization of hydrophobic SBA-15 silicas, J. Colloid Interface Sci. 356 (2011) 690–698, https://doi.org/10.1016/j.jcis.2011.01.033.
[36] Y.V. Kazakevich, A.Y. Fadeev, Adsorption characterization of oligo (dimethylsiloxane)-modified silicas: an example of highly hydrophobic surfaces with non-aliphatic architecture, Langmuir 18 (2002) 3117–3122, https://doi.org/10.1021/la011490r.
[37] N. García, E. Benito, J. Guzmán, P. Tiemblo, Use of p-toluenesulfonic acid for the controlled grafting of alkoxysilanes onto silanol containing surfaces: preparation of tunable hydrophilic, hydrophobic, and super-hydrophobic silica, J. Am. Chem. Soc. 129 (2007) 5052–5060, https://doi.org/10.1021/ja067987a.
[38] S. Cambiaso, F. Rasera, A. Tinti, D. Bochicchio, Y. Grosu, G. Rossi, A. Giacomello, Local grafting heterogeneities control water intrusion and extrusion in nanopores, Commun. Mater. 5 (1) (2024) 1–11, https://doi.org/10.1038/s43246-024-00531-2, 2024 5.
[39] T. Teutenberg, K. Hollebekkers, S. Wiese, A. Boergers, Temperature and pH-stability of commercial stationary phases, J. Separ. Sci. 32 (2009) 1262–1274, https://doi.org/10.1002/jssc.200800712.
[40] K.D. Wyndham, J.E. O'Gara, T.H. Walter, K.H. Glose, N.L. Lawrence, B.A. Alden, G. S. Izzo, C.J. Hudalla, P.C. Iraneta, Characterization and evaluation of C18 HPLC stationary phases based on ethyl-bridged hybrid organic/inorganic particles, Anal. Chem. 75 (2003) 6781–6788, https://doi.org/10.1021/ac034767w.
[41] J. Nawrocki, C. Dunlap, A. McCormick, P.W. Carr, Part I. Chromatography using ultra-stable metal oxide-based stationary phases for HPLC, J. Chromatogr. A 1028 (2004) 1–30, https://doi.org/10.1016/j.chroma.2003.11.052.
[42] H.A. Claessens, M.A. Van Straten, Review on the chemical and thermal stability of stationary phases for reversed-phase liquid chromatography, J. Chromatogr. A 1060 (2004) 23–41, https://doi.org/10.1016/j.chroma.2004.08.098.
[43] T. Teutenberg, J. Tuerk, M. Holzhauser, T.K. Kiffmeyer, Evaluation of column bleed by using an ultraviolet and a charged aerosol detector coupled to a high-temperature liquid chromatographic system, J. Chromatogr. A 1119 (2006) 197–201, https://doi.org/10.1016/j.chroma.2005.12.011.
[44] A. Giacomello, S. Meloni, M. Chinappi, C.M. Casciola, Cassie-baxter and wenzel states on a nanostructured surface: phase diagram, metastabilities, and transition mechanism by atomistic free energy calculations, Langmuir 28 (2012) 10764–10772, https://doi.org/10.1021/la3018453.
[45] A. Le Donne, A. Tinti, E. Amayuelas, H.K. Kashyap, G. Camisasca, R.C. Remsing, R. Roth, Y. Grosu, S. Meloni, Intrusion and extrusion of liquids in highly confining media: bridging fundamental research to applications, Adv. Phys. X 7 (2022), https://doi.org/10.1080/23746149.2022.2052353.
[46] G. Camisasca, A. Tinti, A. Giacomello, Gas-induced drying of nanopores, journal of physical, Chem. Lett. 11 (2020) 9171–9177, https://doi.org/10.1021/acs.jpclett.0c02600.
[47] M. Tortora, S. Meloni, B.H. Tan, A. Giacomello, C.D. Ohl, C.M. Casciola, The interplay among gas, liquid and solid interactions determines the stability of surface nanobubbles, Nanoscale 12 (2020) 22698–22709, https://doi.org/10.1039/D0NR05859A.
[48] A. Giacomello, M. Chinappi, S. Meloni, C.M. Casciola, Metastable wetting on superhydrophobic surfaces: continuum and atomistic views of the cassie-baxter-wenzel transition, Phys. Rev. Lett. 109 (2012) 226102, https://doi.org/10.1103/PhysRevLett.109.226102.
[49] A. Giacomello, S. Meloni, M. Müller, C.M. Casciola, Mechanism of the Cassie-Wenzel transition via the atomistic and continuum string methods, J. Chem. Phys. 142 (2015), https://doi.org/10.1063/1.4913839/76332.
[50] S. Marchio, S. Meloni, A. Giacomello, C.M. Casciola, Wetting and recovery of nano-patterned surfaces beyond the classical picture, Nanoscale 11 (2019) 21458–21470, https://doi.org/10.1039/C9NR05105H.